Australian Earthquake Engineering Society
2023 National Conference, 23-25 November 2023
Brisbane, Queensland, Australia

Constraining fault geometry and slip rates of the Lovely Banks Fault, Victoria

Catherine Peryer[1,2], Brendan Duffy[1,2] and Mark Quigley[2]

1. GHD, 180 Lonsdale Street Melbourne Victoria 3000

2. University of Melbourne, Victoria 3010

Abstract

Topographic analysis of lidar data from the Greater Geelong region of Victoria reveals complex fault geometry and displacement of Quaternary stratigraphy across the Lovely Banks Fault. The reverse fault is traced for a length of 36 km, striking NNE in the south, and NNW along its northern extent, featuring splay faulting and minor backthrusts. A Multichannel Analysis of Surface Waves (MASW) survey suggests a dip of 33° WSW near the surface. Field investigations reveal surface rupturing and the presence of a co-seismic sag pond, post-dating most recent deposition of Quaternary Newer Volcanic Province basalt at Mount Anakie. Fault-perpendicular topographic profiles and restoration of landforms produces maximum Quaternary dip-slip rates associated with broad wavelength deformation of 48.5 (+13.6/-7.6) m/Myr, and local discrete dip-slip rates of 7.6 (+3.4/-2.1) m/Myr. Using fault scaling relationships, we estimate a rupture magnitude of Mw 6.9 (±0.3), with an estimated recurrence rate of 78.7 (+47.8/-24.9) kyr, based on determined Quaternary slip rates and measured displacement.

Keywords: Lidar, neotectonics, slip rates, geomorphology, MASW survey, Lovely Banks Fault.

1 Introduction

Victoria is rapidly urbanizing and cities such as Geelong and Melbourne have growing populations and sprawling infrastructure, making it important to understand the nearby sources of seismic hazard. The limited observation history and relatively sparse seismic network in comparison to the scale of the Australian continent results in large uncertainties associated with our understanding of seismic hazard (Allen et al., 2020; McCue, 2004). On 22 September 2021, the Melbourne region was shaken by the M_W 5.9 Woods Point earthquake, located 130 km from the Melbourne city centre (Quigley et al., 2021). Despite its moderate size and relatively distant location, the shaking damaged buildings in older parts of Melbourne located on relatively weak soils. The damage attests to the impact of built heritage on Melbourne's vulnerability to strong shaking (Wehner et al., 2022) caused by even moderate far field events. Events such as these can occur on faults with lengths in the order of only 3-10 km, which are densely distributed in the Australian crust. However, the Quaternary landscape of the Melbourne volcanic plains (Heath et al., 2020, Che, 2017, Gray & McDougall, 2009) records a

history of larger events, proximal to both Melbourne and Geelong (Figure 1). The earthquake hazard posed by these seismogenic sources is still not well characterised.

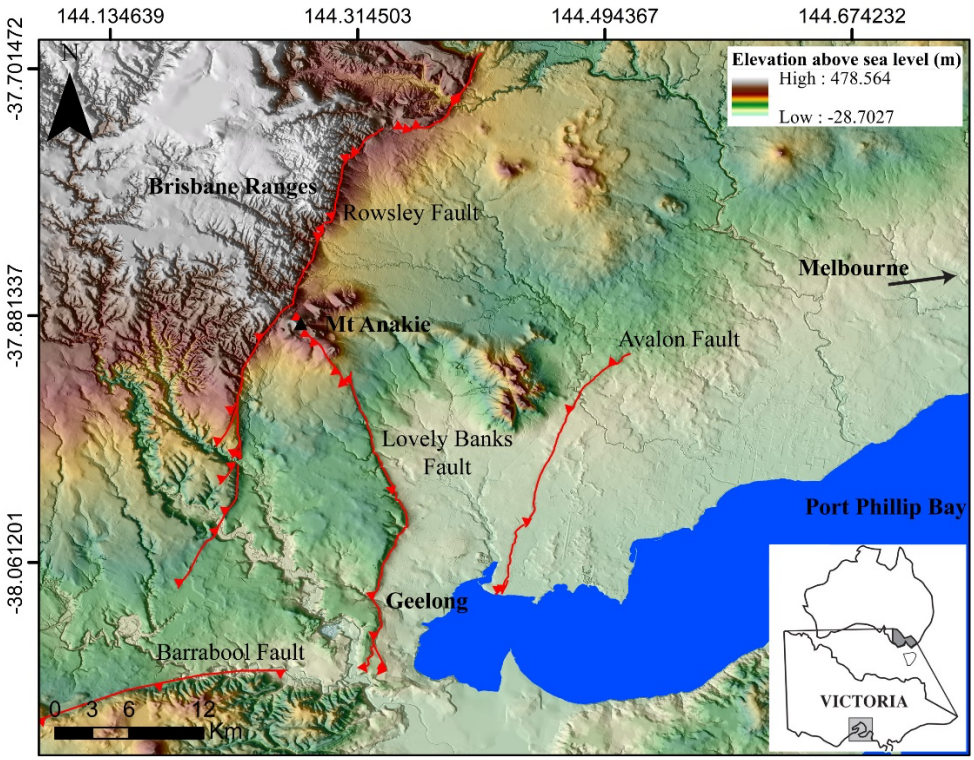

Figure 1 Map of study region highlighting key neotectonic faults.

Three major faults strike generally northwards across the Melbourne volcanic plains north of Geelong. The central fault of this system is known as the Lovely Banks Fault, which has previously been classified as a west-dipping reverse fault (Neotectonic Features Database). Previous studies map the extent of the fault for ~30.6 km, consisting of a NNW striking fault in the north, which curves to strike NNE in the south (Clark & McPherson, 2009; Bowler, 1963). Quaternary Newer Volcanics Province (NVP) basalt is vertically displaced across the fault, and the Moorabool River near Geelong has been diverted by fault uplift, indicating significant seismic activity over Quaternary timescales (Bowler, 1963). Clark and McPherson (2009) provide an estimated maximum vertical slip rate of 35 m/Myr based on a maximum vertical scarp height of 70 m and the age of NVP volcanics dated at ~1.91 to 2.17 Ma by Gibson (2007). This estimate does not account for possible basalt thickness variations across the fault, which could result if a scarp was present in the landscape prior to or during basalt accumulation.

This paper investigates the location, geometry, magnitude, and timing of neotectonic ground-rupturing earthquakes on the Lovely Banks Fault.

2 Geological setting and lithology

The Lovely Banks Fault is located within the Port Phillip Basin in South Victoria (Figure 1). The Port Phillip Basin originated in the Cretaceous, during the period of rifting of Antarctica from Australia that produced the SE Australian continental rift basins (Holdgate et al., 2001; Dickinson et al., 2002). Extensional subsidence of Southeast Australian basins at this time accommodated Paleogene-Miocene sedimentary deposition (Mahon & Wallace, 2020). This was later followed by inversion, significant uplift, and erosion of the Port Phillip Basin from ~12 – 5 Ma, associated with increased contractional strain rates, hypothesized to correlate with

increased loading from the margins of the Australian Plate (Dickinson et al., 2002; Archbold, 1992).

The Port Phillip Basin basement is dominated by Early Ordovician turbiditic Castlemaine Group overlying Cambrian Heathcote Volcanics (Rawling et al., 2011; Archbold, 1992). During the Cenozoic, marine regression and transgression resulted in the deposition of alternating terrestrial and marine sediments respectively (Archbold 1992), interbedded with tuff and basalt from the Older Volcanic eruptions (Holdgate et al. 2002; Archbold, 1992). This is overlain by Pliocene to Quaternary Newer Volcanic Province (NVP) basalts, ranging in eruption age from 4.6 Ma – 5 ka (Gray & McDougall, 2009; Heath et al., 2020; Dickinson et al., 2002).

3 Method

We mapped paleoseismic structures in the study region using lidar-derived 1-5 m resolution digital elevation models (DEMs) provided by Department of Energy, Environment and Climate Action (DEECA), supplemented by 10 m resolution DEMs, geophysical and map datasets, NearMap satellite imagery and published research.

We estimated apparent dip-slip rates from vertical displacement, fault dip and surface age, and accounted for uncertainty by Monte Carlo modelling using the @RISK$_{TM}$ Monte Carlo addin for Excel (https://www.palisade.com/risk/default.asp). We measured net vertical offset of topographic surfaces on scarp-perpendicular profiles where the hanging wall and footwall surfaces were considered to be equivalent based on geomorphic and geological analyses. Estimated best-fit lines of the slope of the relatively undeformed hanging wall and footwall surfaces were projected across the scarp. Vertical offset was then measured as maximum, minimum, and preferred, to accommodate the possible variation in location of fault intersection with the surface. Using measured and estimated fault dip angles, we calculated dip-slip offset across the fault.

The estimated displacement along these profiles is representative of broad wavelength deformation encompassing folding and distributed faulting in the hanging wall.

Ages across the fault were evaluated using geomorphology, eruption centres, nearby published K-Ar ages and age domains (Che, 2017; Gibson, 2007; Gray & McDougall, 2009), and the Australian Stratigraphic Units database. Field measurements for fault dip were used where available, otherwise fault dips were estimated to be 45° ± 15°, incorporating a wide range of fault angle uncertainties, and placed on a normal distribution curve. Dip-slip displacement and rates are given as mode values, representing the peak in the distribution curves. Uncertainties are given as the 95% confidence range.

Fault scaling relationships from Yang et al. (2021) were used in conjunction with measured fault lengths from digital mapping results to estimate earthquake magnitude, fault width, rupture area, and displacement per event. Single-event displacement was then used to estimate average recurrence intervals (assuming constant fault activity), utilising maximum dip-slip displacement across the fault to best capture the central maximum displacement of the fault.

4 Results

Analysis of digital data and field investigations delineates the Lovely Banks Fault for 36 km from the Barwon River in the south to Mt Anakie in the north (Figure 2). In general terms, the fault has two significant sections. The southern section trends NNE for ~12 km before curving

near McNeil Court into a NNW-trending section that extends to Mt Anakie. The western hanging wall has been uplifted significantly, forming a prominent topographic scarp.

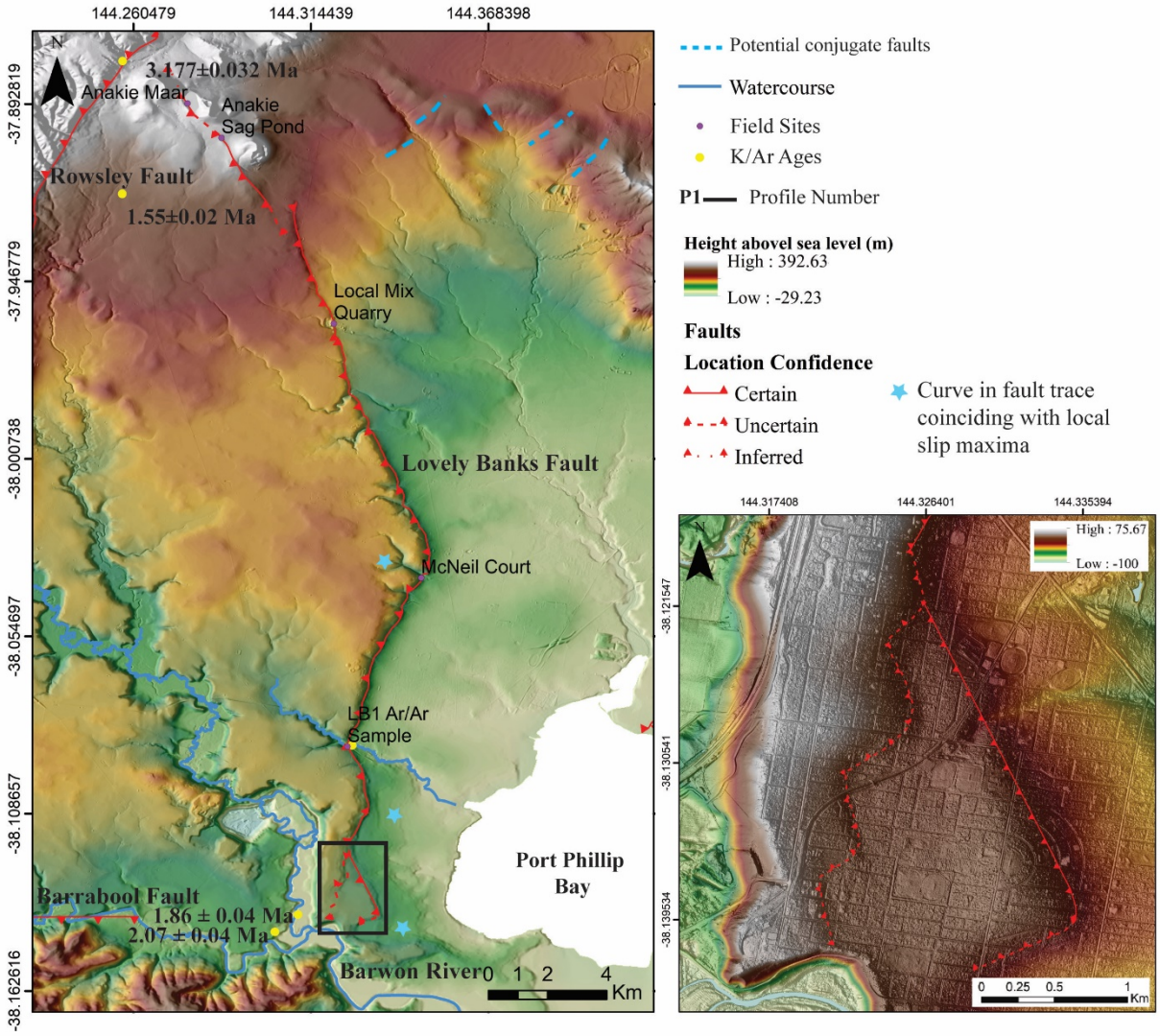

Figure 2- Mapped fault trace with basalt ages.

Much of the fault has a single, clearly defined curving trace. However, at the northern termination of the fault trace, the main trace appears to project east of Anakie while a 6 km long splay fault branches into the hanging wall from the main fault trace. The splay trends ~330° through the Anakie volcanic centres, towards the Rowsley Fault. Field investigations confirm the fault displaces the southwest edge of the Anakie Maar (Figure 2) at an uphill-facing scarp that forms a saddle in the maar rim. There is no evidence for strike-slip visible in the landscape. The preserved offset on the boundary of the maar indicates this fault surface rupture has occurred since the most recent eruption that formed the maar.

The southern end of the Lovely Banks Fault also gains complexity as it approaches the intersection with the generally east-west striking, north-vergent-reverse Barrabool Fault (Figure 2). Over the last 2.5 km, the Lovely Banks Fault splays into its footwall. Meanwhile, the southward continuation of the main trace develops into a series of 500 m-scale, NW-striking, right stepping reverse faults, linked by NE-striking, NW-up transfer structures (inset map, Figure 2). The hanging wall of the Lovely Banks Fault lies mostly in the footwall of the Barrabool Fault (Clark & McPherson, 2009). The mapped Barrabool fault trace terminates west of the Lovely Banks Fault, but projects to intersect the fault; the increased complexity lies

approximately on the projection of that line, where the terminus of the Lovely Banks Fault is effectively incorporated into the Barrabool Fault zone and its hanging wall.

Several structural features provide insight into the orientation of the maximum horizontal stress. High-angle intersections of NNE-and NNW-trending fault traces are observed at three locations on the Lovely Banks Fault (indicated by blue stars, Figure 2). In all three cases, these intersections coincide with surface displacements that are larger than adjacent fault traces. Slip maxima at fault intersections has been observed for several historical Australian earthquakes (e.g., 1986 Marryat Creek, 1968 Meckering (King et al., 2019; Yang et al., 2021)) and may relate to fault intersection lines that are geometrically compatible and optimally oriented with respect to prevailing stress fields (Yang et al., 2021). In this case, these maxima would imply generally E-W oriented S_{Hmax}.

4.1 Anakie sag pond

Analysis of the lidar DEM revealed the possibility of a co-seismic sag pond at the northern-most end of the splay fault, referred to from here on as Anakie sag pond. Figure 3 illustrates the location of a proposed wind gap trending west, likely originating as a westward drainage of the runoff collected between Anakie 2 and 3 volcanic centres. It is likely that the collected rainfall drained to the east and west, until this fault ruptured at an upstream-facing scarp, ponding westward drainage. The accommodation space behind the fault barrier on the footwall filled with ponded water and sediment. The sag pond was eventually drained by headward incision of the eastward draining stream, forming the modern drainage.

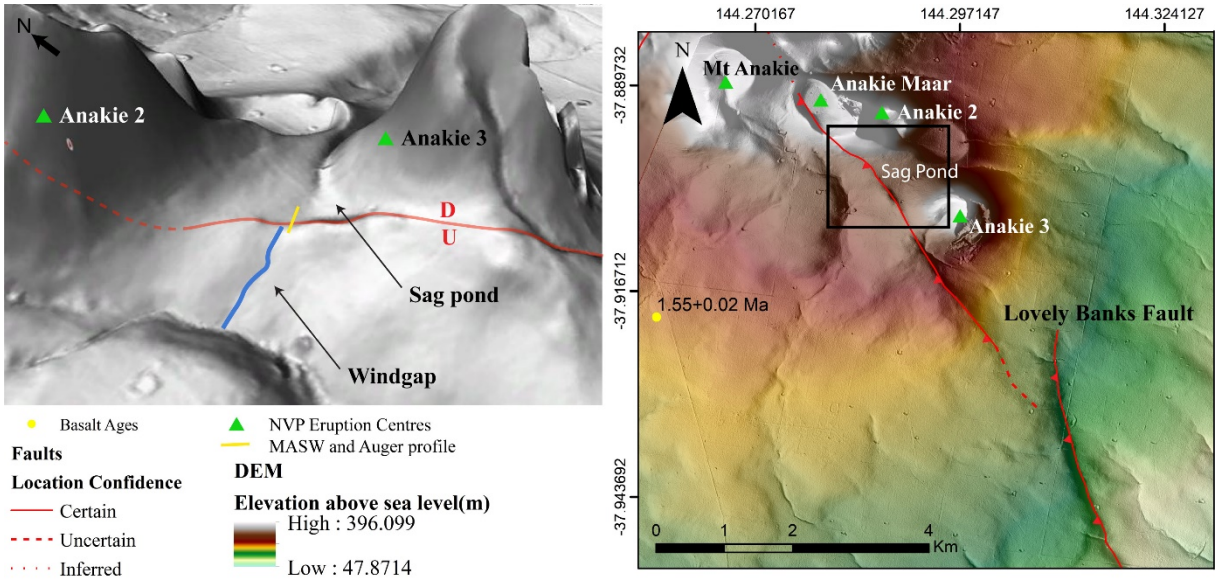

Figure 3 – Anakie sag pond.

Field investigations at the Anakie sag pond site confirmed outcropping basalt on the hanging wall and clay sediment on the footwall of the Lovely Banks Fault. Eleven boreholes were hand augered to refusal to determine depth and origin of sediment overlying the basalt (Figure 3). Excavated clays were interpreted as Quaternary sedimentation, produced from weathering of basaltic detritus deposited in the sag pond environment created by uplift of the hanging wall. A depth profile perpendicular to the fault trace (Figure 4) indicates maximum depth occurring away from the fault scarp, and the sediment shallowing closer to the scarp. This shape suggests some flex or possible drag on the downthrown wall, forming a fault angle depression, or refusal of the auger on coarse colluvium adjacent to the fault.

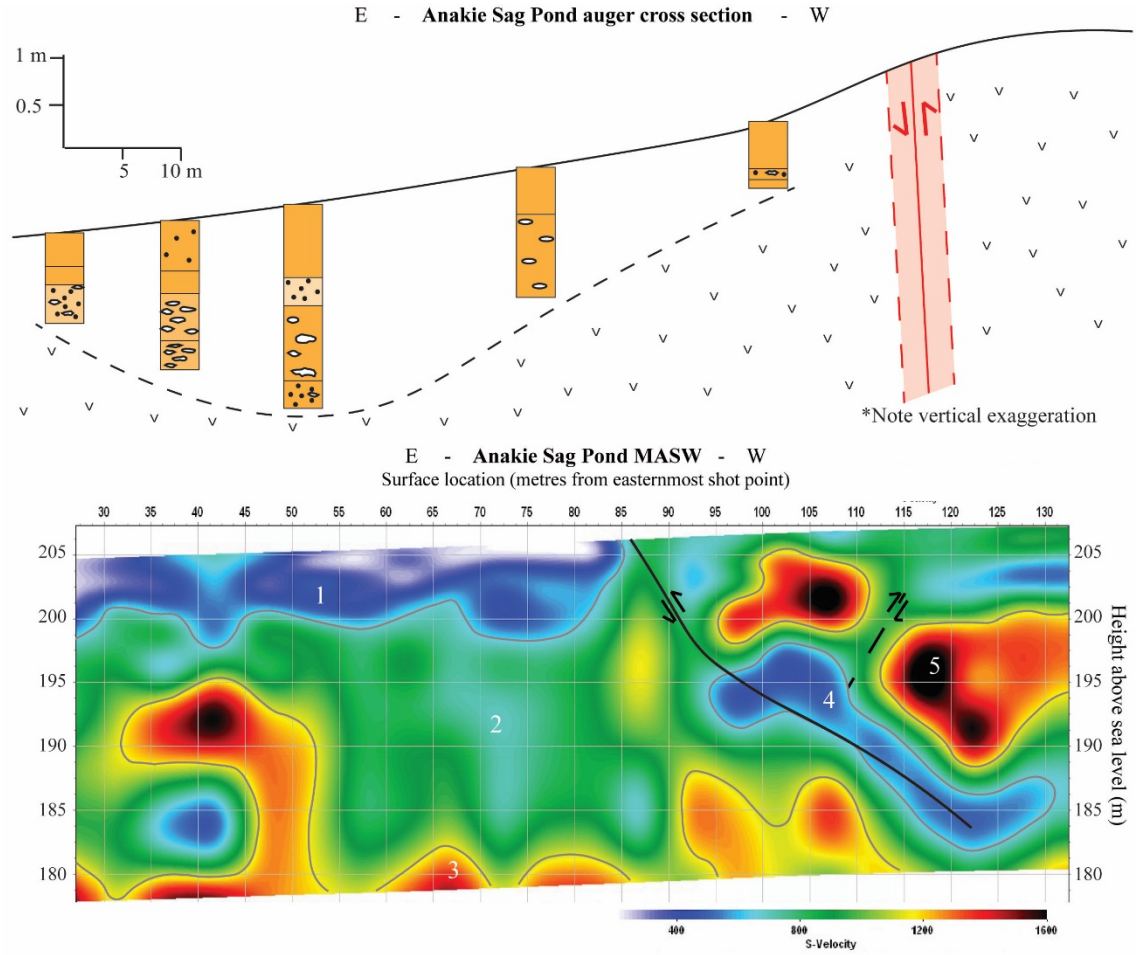

Figure 4 –Fault-perpendicular cross sections at Anakie sag pond. Top - Hand auger results. Bottom - MASW survey profile. (1) Quaternary sedimentation, (2) variably weathered NVP basalt, (3) fresh NVP basalt, (4) shear zone of deformed and fractured NVP basalt, (5) fresh NVP basalt.

4.2 MASW

A MASW survey conducted perpendicular to the fault scarp at the Anakie sag pond site shows a clear depiction of reverse faulting (Figure 4). High shear wave velocity (Vs) close to the surface on the western end of the profile (Loc. 5, Figure 4) are interpreted to show upthrown rigid basaltic material that is exposed at the surface adjacent to the survey line. The underlying Vs inversion at Location 4 (Figure 4), is interpreted as heavily fractured and damaged material associated with the shear zone. Using the dip of this shear zone, the fault trace is estimated to be locally dipping 33°WSW.

The eastern footwall has <5 m of low velocity material (Loc. 1, Figure 4) interpreted as Quaternary sedimentation, likely associated with ponding within the fault angle depression. Underlying this is ~20 m of variably weathered basalt (generally <1000 m/s; Loc. 2, Figure 4), followed by the fresh NVP basalt (typically >1200m/s; Loc. 3, Figure 4). Variations in lateral velocity within the hanging wall may indicate the presence of a small reverse fault producing a pop-up structure with the main fault trace. This interpretation is supported by observations of a structure with similar angle and context observed in outcrop at the Local Mix Quarry (Figure 2).

4.3 Slip rates

Vertical offset across the fault at the Anakie sag pond is estimated to be 5 to 8 m. However, the surface expression of the fault scarp here is < 3 m, indicating significant sedimentation occurred within the sag pond since the most recent rupture event. The closest dated basalt flow is 1.55 ± 0.02 Ma located just south of Mt Anakie (Figure 2). It is likely that this basalt flow originated from one of the Anakie eruption centres, covering this site prior to faulting, indicating that faulting and sag pond formation post-date the basalt flow. Using the 33°WSW fault dip observed at this location, we calculate a local dip-slip displacement of 11.8 (+3.2/-2.6) m and a dip-slip rate of 7.6 (+3.4/-2.1) m/Myr. These estimates are representative of local discrete displacement against the fault.

Figure 5 depicts vertical offset profiles generated across the fault scarp south of Anakie. Profiles are drawn where NVP basalt is present on both sides of the fault scarp, and used to estimate the best-fit slope of the relatively undeformed surface. The thickness of basalt is poorly constrained either side of the fault, due to scarcity of boreholes, and shallow depth of drilling. Field investigations revealed basalt at the Local Mix Quarry site (Figure 2) is as thick as 40 m in the proximal hanging wall, however it is not known if the flow is equally thick on the footwall. It is therefore possible that 1) the scarp was in place during basalt deposition, resulting in uneven distribution of basalt laterally - in this case, estimated slip rates could over-estimate the true fault slip rate; 2) the landscape was relatively flat during NVP emplacement, resulting in basalt flow covering the whole region relatively evenly. In this case the estimated dip-slip rates for the post-NVP basalt period will more accurately reflect Quaternary displacement; 3) the fault ruptured during the magmatic episode, producing a combination of 1 and 2 (e.g., Duffy and Dimas, 2022), in which case lava may have pooled on the footwall and topographic displacement underestimates the dip-slip displacement. We note that the extension of the Miocene-Pliocene strandplain across this region (Wallace et al., 2005) supports a relatively flat landscape prior to NVP basalt deposition.

The age of the NVP basalt surface across all profiles is estimated from the closest K-Ar basalt ages (Figure 2), where dated flows show consistent geomorphic character that suggests they cover the profiled offset surface. Where ages are not well constrained due to the sparse dating sites, regional dating domains described by Gray and McDougall (2009) are used.

Table 1 displays the results of @RISK$_{TM}$ dip-slip displacement and dip-slip rate calculation. The broad fault scarp indicates a wide zone of folding on the hanging wall accompanies the main fault displacement. Estimates of displacement and slip rates across the scarp using topographic profiles are therefore representative of broad wavelength deformation across the system. The greatest displacement occurs at the centre of the fault trace (represented by Profile 2, Figure 5), where the NNE-and NNW-trending fault traces intersect. Offset decreases progressively northwards, as the fault trace curves NNW and becomes oblique to S_{Hmax}. Slip rates follow the same spatial pattern. Where the main fault trace terminates in the north and the linking fault branches towards the NW, the fault displacement and slip rate are significantly reduced. Basalt ages in the region are sparse and variable; this uncertainty in age is reflected via propagation into the uncertainties in the fault slip rates.

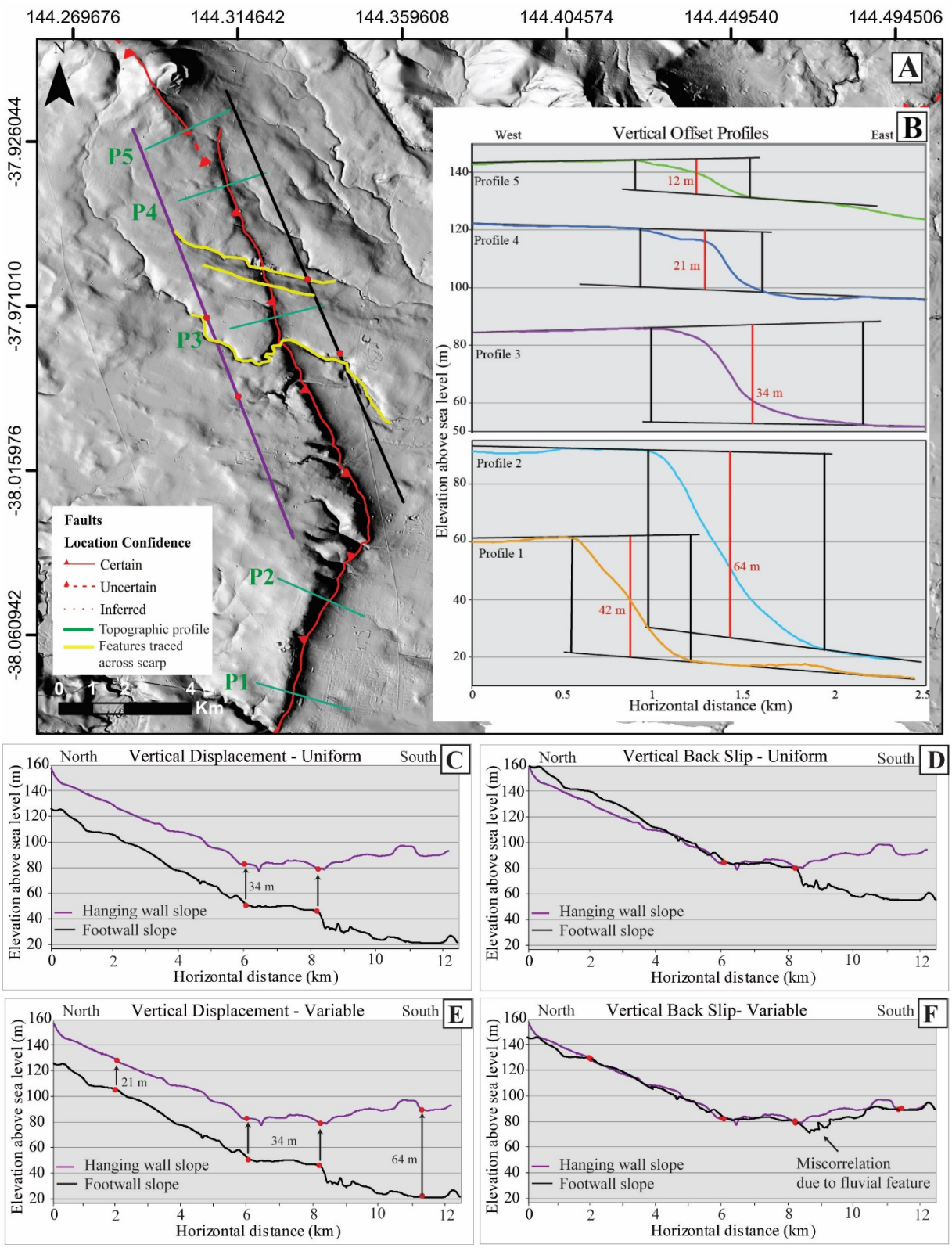

Figure 5- Lovely Banks Fault topographic profile analyses. B – Fault-perpendicular topographic profiles illustrating broad wavelength displacement deformation. Black sub-horizontal lines represent interpreted slope of the relatively undeformed NVP basalt surface. Vertical lines represent minimum, maximum and preferred (red) measurements of apparent vertical displacement. C and D - Uniform vertical back-slip using vertical offset from Profile 3. E and F – Variable vertical back-slip using vertical offset from profiles 2-4.

Table 1 - Quaternary dip-slip displacement and slip rate results produced using @RISK™ software.

	Profile number	Dip-slip displacement (m)	Dip-slip rate (m/Myr)
Broad wavelength deformation*	Profile 1	57.5 (+15.1/-6.6)	31.4 (+8.8/-4.9)
	Profile 2	89.9 (+22.3/-11.6)	48.5 (+13.6/-7.6)
	Profile 3	47.65 (+12.5/-5.5)	30.4 (+14/-5.9)
	Profile 4	28.8 (+7.2/-3.4)	19.1 (+7.6/-4.3)
	Profile 5	17.0 (+4.3/-2.7)	10.5 (+5.2/-2)
Discrete displacement**	Anakie sag pond	11.8 (+3.2/-2.6)	7.6 (+3.4/-2.1)

*Using estimated fault dip of 45º (±15)
**Using measured local fault dip of 33º (±5)

4.4 Back slipping

The northern segment of the Lovely Banks Fault is oriented obliquely to the contemporary S_{Hmax} of NW-SE (Rajabi et al., 2017) suggesting that a component of strike-slip movement on the fault is possible. This was investigated using features crossing the scarp and back slipping techniques.

Figure 5A illustrates three landscape features that are crossing the scarp, none of which demonstrate lateral offset. The pervasive regional slope towards the SE into the centre of the Port Phillip Bay, is causing streams to trend predominantly SE. The meandering of the stream channel on the hanging wall near the centre of the fault highlights the local dip-slip maxima that is occurring at the centre of the fault trace, compensating for the regional slope, and making a near-flat topography here (Figure 5C). Any strike-slip movement on this fault would be expected to cause lateral offset in these highlighted features.

To further evaluate whether there is any evidence of strike-slip on the Lovely Banks Fault, fault-parallel profiles were restored (back-slipped) using the estimated vertical offset determined above. Figure 5 illustrates two methods of back-slipping, using uniform and variable vertical offset across the profile. Figure 5C and 5D identifies two points of change in slope on both profiles, and uniformly back-slips the profile 34 m (derived from Profile 3 vertical offset estimates). This method fails to realign the slopes on either side of the plateau, due to a variation in slip rates present across the scarp. Figure 5E and 5F identifies multiple points across the profiles, corresponding to the vertical offset estimates from Profiles 2-4, and realigns the profiles using variable vertical offset. This technique successfully restores the landscape using only vertical back-slip, indicating that pure dip-slip can restore the landscape, and there is no apparent element of strike-slip present on the fault.

4.5 Fault scaling relationships

Earthquake parameters (Table 2) are estimated from Yang et al. (2021) fault scaling relationships. These results assume periodic characteristic earthquakes, estimated from the largest dip-slip displacement and dip-slip rates towards the central region of each fault trace, to estimate maximum magnitude and recurrence rates. These results are calculated from Quaternary displacement estimates and may not be reflective of older fault activity.

The estimated and maximum magnitude rupture values represent the variability between an elliptical rupture patch that is tangential to the surface, and a rupture patch that extends throughout the seismogenic zone and intersects the surface along the full fault trace.

Table 2 - Estimated fault rupture characteristics.

SRL (km)	M_w [0]	Seismogenic thickness (km)	Max W (km @ 45° dip)	Max A[1] (km^2)	Max M_W[2]	Dav[0] (m)	Dip-slip rate[3] (m/Myr)	Average recurrence interval[4] (kyr)
35.5	6.9 (±0.3)	12.0	17	480	7.3 (±0.1)	3.9 (+2/-1)	48.5 (+13.6/-7.6)	78.7 (+47.8/-24.9)

[0] Calculated from relationship in Yang et al., (2021). Lower bounds would imply only c.3km wide full length rupture.
[1] Calculated as half ellipse intersecting full surface trace and full width of seismogenic zone.
[2] Calculated from μAD with μ=3GPa, generally consistent with upper bounds of Yang et al. relationship.
[3] Calculated on 45° dipping fault.
[4] Calculated from dip slip rate, and single event dip slip at sag pond.

5 Discussion

Digital mapping of the Lovely Banks Fault reveals extension of the branching northern fault trace through the Anakie volcanic centres to almost intersect the Rowsley Fault. Field investigations confirm the presence of a reverse fault (dipping 33° at 0-20 m depth) as proposed in the literature.

Maximum slip rates of 48.5 (+13.6/-7.6) m/Myr in the central section of the fault are representative of broad wavelength deformation, and exceed the 35 m/Myr estimate by Clark and McPherson (2009). These measurements inform an estimated periodic characteristic earthquake surface rupture event of M_W 6.9 every ~79,000 years, assuming a constant activity rate on the fault. A possible maximum M_W 7.3 represents a fault rupture through the full 12 (±3) km seismogenic thickness of southeastern Australia. Basalt thickness across the fault is poorly constrained, making it difficult to ascertain whether the dip-slip displacement visible in the landscape can be totally attributed to offset of NVP basalt. It is possible that Quaternary dip-slip is overestimated due to a pre-existing fault scarp, or underestimated due to differential basalt pooling on the footwall.

A slip rate of 7.6 (+3.4/-2.1) m/Myr is derived from fault geometry and stratigraphy revealed by MASW survey. This slip rate is representative of discrete displacement against the fault, however 1) it is situated in a zone of diminished displacement near the fault terminus, and is therefore not applicable to the total fault scarp; 2) it is measured on a splay that captures only part of the slip budget. Additional boreholes on either side of the scarp could help constrain pre-Quaternary topography and improve confidence in slip rates on the Lovely Banks Fault.

Preservation of the fault scarp within the Anakie Maar indicates that Quaternary surface rupture has occurred on the fault. This is further supported by MASW survey results that illustrate surface rupture of Quaternary stratigraphy, and the exposure of faulted NVP basalt to the surface in the Local Mix Quarry outcrops.

6 Conclusion

The Lovely Banks Fault is 36 km long, striking NNE in the south, and NNW in its northern extent, featuring a splay fault trace and backthrusts. A MASW survey suggests a dip of 33°WSW near the surface. MASW surveys and field observations indicate a smaller reverse fault on the hanging wall, branching at depth from the main fault trace to form a pop-up

structure. The broad wavelength slip rate of 48.5 (+13.6/-7.6) m/Myr measured across the centre of the scarp is assumed to be a minimum estimate, due to the possibility of uneven basalt accumulation across the scarp. Fault scaling relationships suggest Quaternary fault rupture events of maximum M_W 6.9 (±0.3) on average every 78.7 kyr (+47.8 kyr, -24.9 kyr). A MASW survey provides evidence of neotectonic surface rupture of Quaternary sediments.

7 Future work

This study identifies the Anakie sag pond site as a potential paleoseismic trenching location. Future trenching of this site may reveal tectonically-disturbed sediments, which when dated could constrain ages of most recent activity on this fault, and further refine local slip rates.

8 Acknowledgements

The authors would like to thank the AEES for their award of the 2020 Charles Bubb Scholarship that funded this research. We are grateful to the Wadawurrung Traditional Owners for their time, effort and partnership in consultation about paleoseismic trenching works on Wadawurrung traditional land, and to Andrew Browne for allowing us access to his property in Anakie.

9 References

Allen, T.I., Griffin, J.D., Leonard, M., Clark, D.J., and Ghasemi, H. (2020). The 2018 national seismic hazard assessment of Australia: Quantifying hazard changes and model uncertainties, Earthquake Spectra, vol. 36, pp. 5-43.

Archbold, N.W. (1992). Outline of the stratigraphy of the Melbourne region, in WA Peck, JL Neilson, RJ Olds, & KD Seddon (eds), Engineering geology of Melbourne, AA Balkema, Rotterdam, Brookfield, pp. 3-8.

Bowler, J. (1963). Port Phillip Survey 1957-1963: The geology and geomorphology. Department of Geology, University of Melbourne, 63, pp.19-67.

Che, X. (2017). Constraints on the eruption history of Basalt in the Bacchus Marsh region of the Newer Volcanic Province, Victoria, Masters Thesis, University of Melbourne, Melbourne.

Clark, D., and McPherson, A. (2009). Potential sources of strong ground shaking within ~200 km of the Otways CCS site, unpublished report, Geoscience Australia.

Dentith, M.C., and Featherstone, W.E. (2003). Controls on intra-plate seismicity in southwestern Australia, Tectonophysics, vol. 376, pp. 167-184.

Dickinson, J.A., Wallace, M.W., Holdgate, G.R., Daniels, J., Gallagher, S.J., and Thomas, L. (2001). Neogene tectonics in SE Australia: implications for petroleum systems, The APPEA Journal, vol. 41, pp. 37-52.

Dickinson, J.A., Wallace, M.W., Holdgate, G.R., Gallagher, S.J., and Thomas, L. (2002). Origin and timing of the Miocene-Pliocene unconformity in southeast Australia, Journal of Sedimentary Research, vol. 72, no. 2, pp. 288-303.

Duffy, B., and Dimas, V-A. (2022). The challenge of characterising earthquakes in a dormant volcanic field, Queensland, Australia, in Australian Earthquake Engineering Society Conference 2022, Nov 24-25, Mt Macedon, Vic.

Gibson, D.L. (2007). Potassium–argon ages of late Mesozoic and Cainozoic igneous rocks of Eastern Australia, CRC LEME Open File Report 193, CSIRO, Kensington, Western Australia.

Gray, C.M., and McDougall, I. (2009). K-Ar geochronology of basalt petrogenesis, Newer Volcanic Province, Victoria, Australian Journal of Earth Sciences, vol. 56, no. 2, pp. 245-258.

Heath, M., Phillips, D. and Matchan, E.L. (2020). Basalt lava flows of the intraplate Newer Volcanic Province in south-east Australia (Melbourne region): 40Ar/39Ar geochronology reveals~ 8 Ma of episodic activity, Journal of Volcanology and Geothermal Research, vol. 389, pp. 106730.

Holdgate, G.R., Gallagher, S.J., and Wallace, M.W. (2002). Tertiary coal geology and stratigraphy of the Port Phillip Basin, Victoria, Australian Journal of Earth Sciences, vol. 49, no. 3, pp. 437-453.

Holdgate, G.R., Geurin, B., Wallace, M.W., and Gallagher, S.J. (2001). Marine geology of Port Phillip, Victoria, Australian Journal of Earth Sciences, vol. 48, no. 3, pp. 439-455.

King, T.R., Quigley, M., and Clark, D. (2019). The 30th March 1986 Mw 5.7 Marryat Creek surface rupturing earthquake, Australia, EarthArXiv.

McCue, K. (2004). Australia: historical earthquake studies, Annals of Geophysics, vol. 47, no. 2/3, pp. 387-397.Rajabi, M., Tingay, M., Heidbach, O., Hillis, R. and Reynolds, S. (2017). The present-day stress field of Australia, Earth-Science Reviews, vol. 168, pp. 165-189.

Neotectonic Features Database, viewed November 2023, <https://neotectonics.ga.gov.au/>.

Quigley, M., Pascale, A., and Allen, T. (2021). Wednesday 22 September 2021 Mw 5.9 Woods Point earthquake information sheet, Earthquake Engineering Research Institute – Australian Earthquake Engineering Society – New Zealand Society of Earthquake Engineering Joint Learning From Earthquakes Clearinghouse.Rawling, T.J., Osbourne, C., McLean, M.A., Skladzien, P.B., Cayley, R.A. and Williams, B. (2011). 3D Victoria final report, GeoScience Victoria 3D Victoria Report 14, Department of Primary Industries.

Wallace, M., Dickinson, J.A., Moore, D.H., and Sandiford, M. (2005). Late Neogene strandlines of southern Victoria: a unique record of eustasy and tectonics in southeast Australia, Australian Journal of Earth Sciences, vol. 52, no. 2, pp. 279–297.

Wehner, M., Ryu, H., Edwards, M., Butt, S., Juskevics, V., Vaculik, J., Mohanty, I., Griffith, M., Hewison, R., Corby, N., and Allen, T. (2022). Melbourne CBD Case Study: URM Retrofit Effectiveness in Avoiding Mass Casualties, in Australian Earthquake Engineering Society Conference 2022, Nov 24-25, Mt Macedon, Vic.

Yang, H., Quigley, M., and King, T. (2021). Surface slip distributions and geometric complexity of intraplate reverse-faulting earthquakes, GSA Bulletin, vol. 13, pp. 1909-1929.